AD-A114 716 MASSACHUSETTS INST OF TECH CAMBRIDGE F/G 11/6
FCC AND BCC SOLIDIFICATION PRODUCTS IN A RAPIDLY SOLIDIFIED AUS--ETC(U)
DEC 81 T F KELLY, J B VANDER SANDE, M COHEN N00014-81-K-0013
UNCLASSIFIED TR-3 NL

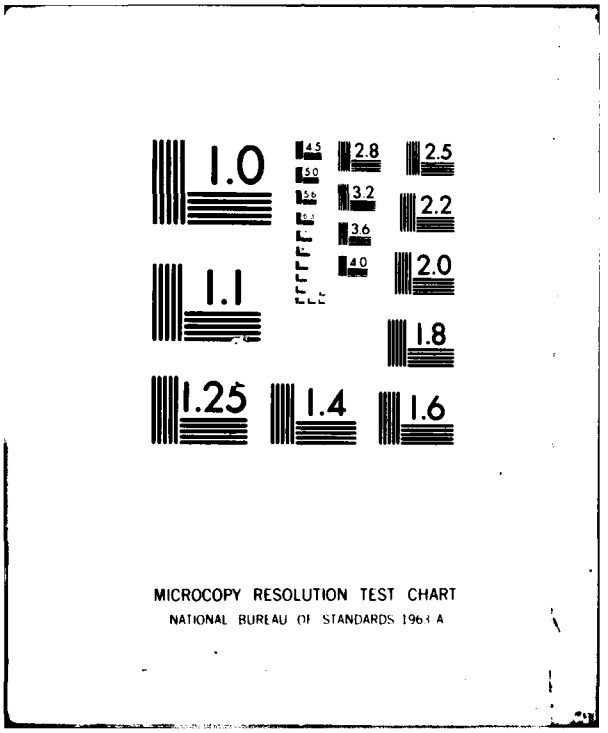
1.0
1.1
1.25
1.4
1.6
1.8
2.0
2.2
2.5
2.8
3.2
3.6
4.0
4.5
5.0
5.6
6.3
7.1
MICROCOPY RESOLUTION TEST CHART
NATIONAL BUREAU OF STANDARDS 1963 A

SECURITY CLASSIFICATION OF THIS PAGE (When Data Entered)

RECD MAY 10 1982

REPORT DOCUMENTATION PAGE

READ INSTRUCTIONS BEFORE COMPLETING FORM

1. REPORT NUMBER: Technical Report No. 3, 1980-81	2. GOVT ACCESSION NO.: AD-A114716
3. RECIPIENT'S CATALOG NUMBER:	
4. TITLE (and Subtitle): "FCC and BCC Solidification Products in a Rapidly Solidified Austenitic Steel"	5. TYPE OF REPORT & PERIOD COVERED: Technical; Oct. 1980 - Sept. 1981
	6. PERFORMING ORG. REPORT NUMBER:
7. AUTHOR(s): Thomas F. Kelly, John B. Vander Sande and Morris Cohen	8. CONTRACT OR GRANT NUMBER(s): N00014-81-K-0013
9. PERFORMING ORGANIZATION NAME AND ADDRESS: Massachusetts Institute of Technology, Cambridge, Massachusetts 02139	10. PROGRAM ELEMENT, PROJECT, TASK AREA & WORK UNIT NUMBERS:
11. CONTROLLING OFFICE NAME AND ADDRESS: Office of Naval Research, Arlington, VA 22217	12. REPORT DATE: 1 December 1981
	13. NUMBER OF PAGES: 6
14. MONITORING AGENCY NAME & ADDRESS (if different from Controlling Office): MCIC-CAB DISTRIBUTION Reviewer Dat Used Reject	15. SECURITY CLASS. (of this report): Unclassified
	15a. DECLASSIFICATION/DOWNGRADING SCHEDULE:

16. DISTRIBUTION STATEMENT (of this Report)

Unlimited

17. DISTRIBUTION STATEMENT (of the abstract entered in Block 20, if different from Report)

18. SUPPLEMENTARY NOTES

To be published in Proceedings of Materials Research Society Symposium on Rapidly Solidified Crystalline and Amorphous Materials, held in Boston on November 17-19, 1981.

19. KEY WORDS (Continue on reverse side if necessary and identify by block number)

Rapid solidification, stainless steels, scanning transmission electron microscopy, metastable phase synthesis

20. ABSTRACT (Continue on reverse side if necessary and identify by block number)

The microstructures and local composition variations in centrifugally atomized high-sulfur stainless steel powder are investigated. Both fcc and bcc are found to be primary solidification phases in the as-solidified powder of this nominally austenitic steel where the smaller powder particles (≤70 micron diameter) tend to be bcc. Cellular solidification structures, with sulfide precipitates (100 to 200 nm diameter in size) at the cell walls, are observed in both fcc and bcc particles. The bcc structure, however, has many small sulfide precipitates (10 to 20 nm diameter) in the cell interior with few-

DD FORM 1 JAN 73 1473 EDITION OF 1 NOV 65 IS OBSOLETE S/N 0102-014-6601

SECURITY CLASSIFICATION OF THIS PAGE (When Data Entered)

larger sulfide precipitates at the cell walls. The small precipitates, observed only in the bcc structures, form on cooling from a supersaturated solid solution that results from reduced solute partitioning during solidification. Partitioning of chromium and nickel is minimal in these cellular structures. A non-cellular bcc structure is also observed with small sulfide precipitates throughout the entire structure. This non-cellular bcc structure results from smooth-front massive solidification. Analysis of the nucleation process for solidification indicates that a transition from fcc nucleation to bcc nucleation occurs with increasing wetting angle in heterogeneous nucleation Thus bcc should nucleate in the smaller droplets of a liquid dispersion where catalytic surfaces of low potency (large wetting angle) tend to be the only heterogeneous nucleants available.

FCC AND BCC SOLIDIFICATION PRODUCTS IN A RAPIDLY SOLIDIFIED AUSTENITIC STEEL.

THOMAS F. KELLY, JOHN B. VANDER SANDE AND MORRIS COHEN
Department of Materials Science and Engineering, M.I.T., Cambridge, Massachusetts 02139

ABSTRACT

The microstructures and local composition variations in centrifugally atomized high-sulfur stainless steel powder are investigated. Both fcc and bcc are found to be primary solidification phases in the as-solidified powder of this nominally austenitic steel where the smaller powder particles ($\lesssim$ 70 micron diameter) tend to be bcc. Cellular solidification structures, with sulfide precipitates (100 to 200 nm diameter in size) at the cell walls, are observed in both fcc and bcc particles. The bcc structure, however, has many small sulfide precipitates (10 to 20 nm diameter) in the cell interior with few larger sulfide precipitates at the cell walls. The small precipitates, observed only in the bcc structures, form on cooling from a supersaturated solid solution that results from reduced solute partitioning during solidification. Partitioning of chromium and nickel is minimal in these cellular structures. A non-cellular bcc structure is also observed with small sulfide precipitates throughout the entire structure. This non-cellular bcc structure results from smooth-front massive solidification. Analysis of the nucleation process for solidification indicates that a transition from fcc nucleation to bcc nucleation occurs with increasing wetting angle in heterogeneous nucleation. Thus bcc should nucleate in the smaller droplets of a liquid dispersion where catalytic surfaces of low potentcy (large wetting angle) tend to be the only heterogeneous nucleants available.

EXPERIMENTAL PROC[illegible]

An austenitic [illegible]nless steel* was rapidly solidified‡ by centrifugal atomization and forced convective cooling in helium at cooling rates on the order of 10^5 K/s and greater. Electron-transparent specimens of the powder were prepared from composite foils of powder in electrodeposited nickel by a combination of conventional jet electropolishing and ion beam milling. Specimens were observed in scanning transmission electron microscopy where compositions are determined by analysis of X-ray fluorescence spectra. For more details see Reference 1.

*Nominal composition wt%

Fe	Cr	Ni	Mn	Cu	Si	Mo	S	Co	C	N	P
bal	17.3	8.7	1.60	0.78	0.66	0.37	0.34	0.17	0.034	0.032	0.028

‡The powders were kindly supplied by Pratt and Whitney Aircraft Group, Government Products Division, United Technologies Corporation, West Palm Beach, Florida 33402.

RESULTS

Both fcc and bcc structures are found in the rapidly solidified powder of t 303 stainless steel. In the as-solidified powder which is sieved to -140 mesh ($\sim$ 120 micron diameter), fcc is the primary solidification phase in the larger particles ($\sim$ 70 micron diameter) and bcc is the primary solidification phase i the smaller particles ($\sim$ 70 μm diameter). Secondary electron micrographs (SEM) of the magnetically separated particles, Figure 1, clearly show the relative sizes of the fcc and bcc particles. The bcc particles account for about 15% by weight of the sieved powder.

Microstructures

Cellular solidification structures are observed in both the fcc and bcc particles. A non-cellular solidification structure, which is the result of a smooth-front massive solidification, is observed in the bcc particles only.

The microstructure and associated composition profile of an fcc cellular structure, Figure 2, shows remnants of solute partitioning during cellular solidification. Precipitate particles, nominally manganese sulfide, on the order of 100 to 200 nm diameter, form at the cell walls at the late stages of solidification from an intercellular fluid enriched in manganese and sulfur. Although the structure is nearly homogeneous with respect to chromium, nickel, and iron, some enrichment of nickel and depletion of iron is observed at the cell walls of the structure.

There is almost no partitioning of solute in the bcc cellular solidification structure, Figure 3. The compositions of chromium, iron and nickel are essentially uniform in the structure. The volume fraction of precipitate particles at the cell walls in this bcc cellular structure is greatly reduced as compared to the fcc cellular structure. Instead, very small (10 to 20 nm diameter) precipitate particles, again nominally manganese sulfide, reside in the cell interiors. These small precipitates are apparently the result of solid-state precipitation.

The bcc non-cellular solidification structure has solidified with no apparent solute partitioning. This phenomenon can be considered as massive solidification. The structure is uniform and compositionally homogeneous throughout, Figure 4. Entire bcc non-cellular particles are observed with a fine dispersion of the very small (10 to 20 nm diameter) precipitates. High temperature heat treatments and available thermodynamic data[3] indicate that no high-temperature solid single phase exists for this alloy. Massive solidification of this alloy to the bcc structure therefore directly produced a solid solution that was supersaturated with respect, at least, to the precipitate forming elements manganese and sulfur.

Origins of FCC and BCC

The origin of the bcc solidification structures in the smallest particles of the powder, has been analyzed[2] for this 303 stainless steel alloy that normally solidifies as fcc from bulk liquids. Using calculated values of the entropy of fusion and a theoretical estimate of the liquid/solid surface tension normalized to the heat of fusion for fcc and bcc[4,5], the temperature at which nucleation of a given solid phase will occur in the liquid droplets is calculated. In Figure 5, this expected nucleation temperature of the fcc and bcc structures is shown as a function of wetting angle in heterogeneous nucleation. Note that the decrease of the fcc nucleation temperature with increasing wetting angle is more rapid than that of bcc and the plots for fcc and bcc cross with increasing wetting angle. When potent heterogeneous nucleants (low wetting angle) are available, fcc structures should nucleate at small liquid supercoolings. If,

however, the more potent heterogeneous nucleants are isolated into a limited number of liquid droplets, which will tend to be the larger droplets, then greater liquid supercoolings will result. Thus bcc structures should nucleate on the heterogeneous nucleants of lower potency which are the only nucleants available in the smaller liquid droplets.

DISCUSSION

The production of a solid solution, supersaturated with respect to precipitate-forming elements, by massive solidification is significant in that it suggests a possible process route for production of precipitation strengthened alloys that cannot be produced by solid state processing. In effect, the liquid is used as the high temperature single phase of high solubility.

Whether solidification to a bcc structure is a necessary ingredient for production of a supersaturated solid solution by massive solidification has not been demonstrated for this alloy. It is possible that fcc would solidify massively if it were to form at the greater liquid supercoolings. There may, however, in some circumstances be significant advantages to solidifying to crystal structures which are secondary nucleation phases, such as bcc relative to fcc.

The necessity of dispersing the liquid in order to achieve effective isolation of the more potent heterogeneous nucleants indicates that secondary and tertiary, etc.,nucleation phases will only be produced in processes that atomize the liquid or otherwise form small liquid volumes. Likewise, high cooling rates during solidification, though important for maintenance of high solid growth rates and for rapid quenching from high temperatures, are not necessary for production of secondary nucleation phases.

CONCLUSIONS

Both fcc and bcc are primary solidification phases in the small liquid droplets of 303 stainless steel. Suppression of solute partitioning in 303 stainless steel has occurred; a) with respect to chromium and nickel in the rapid solidification of fcc structures and b) with respect to chromium, nickel, manganese and sulfur in the rapid solidification of bcc structures. Massive solidification of bcc structures results in a supersaturated solid solution with respect to the precipitate forming elements manganese and sulfur. This supersaturated solid solution cannot be obtained by solid state processing of this alloy.

Nucleation of the solid is the structure-determining step in the solidification of the liquid droplets. The bcc structure appears primarily in the smaller particles due to isolation of the more potent heterogeneous nucleants, which tend to catalyse fcc nucleation, into a limited number of liquid droplets.

ACKNOWLEDGEMENTS

The authors are grateful for the financial support provided by the Office of Naval Research, Contract number N00014-81-K-0013. Special thanks are extended to C. V. Thompson and F. Spaepen for fruitful discussions and for providing results of their unpublished research.

REFERENCES

1. Thomas F. Kelly, John B. Vander Sande and Morris Cohen; "Rapid Solidification of a Stainless Steel: Partl-Suppressed Partitioning and Supersaturated Solid Solutions in FCC and BCC Solidification Products." to be published.

2. Thomas F. Kelly, John B. Vander Sande and Morris Cohen; "Rapid Solidification of a Stainless Steel: Part 2-Origins of FCC and BCC Solidification Products.", to be published.

3. E. T. Turkdogan, S. Ignatowicz and J. Pearson; JISI, 180, 349 (1955).

4. F. Spaepen and R. B. Meyer; Scripta Met., 10, 257 (1976).

5. C. V. Thompson and F. Spaepen, to be published.

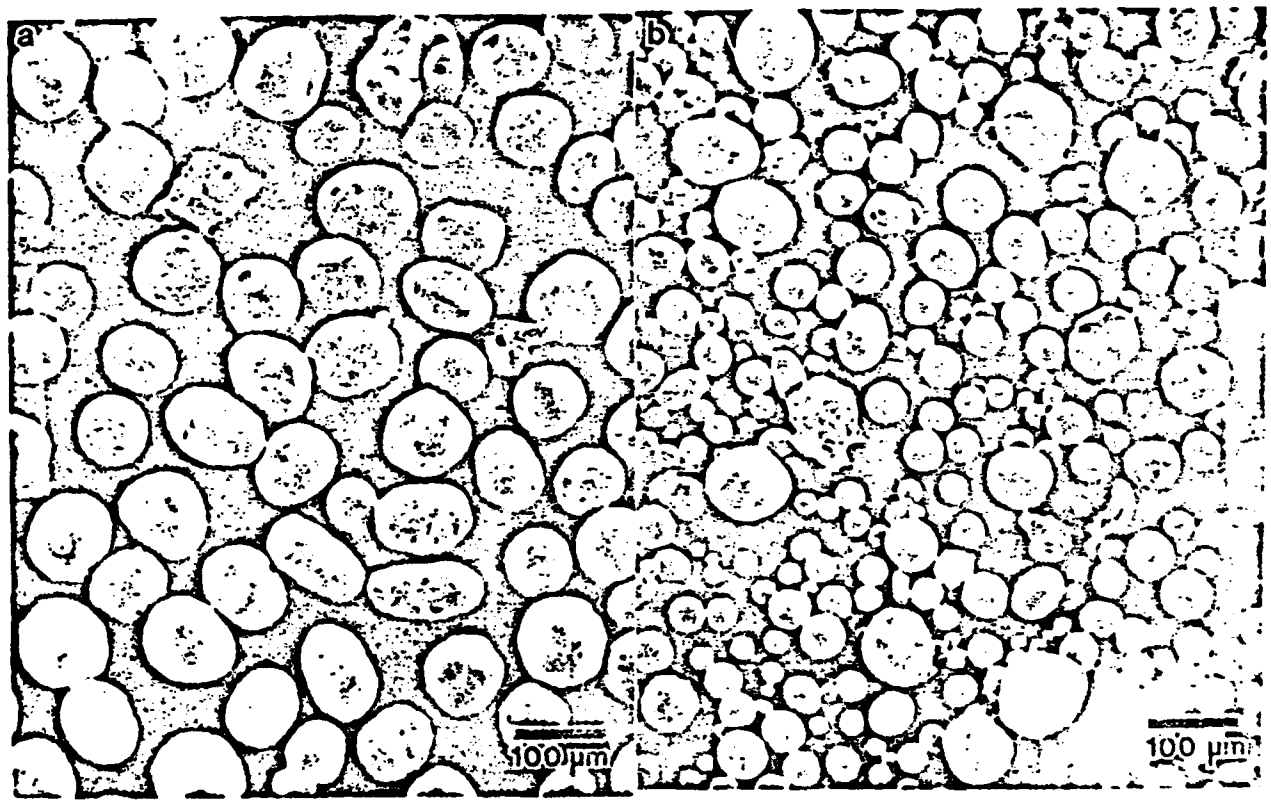

Figure 1 - Rapidly solidified powder of 303 stainless steel. Secondary electron images of a) non-ferromagnetic and b) ferromagnetic particles.

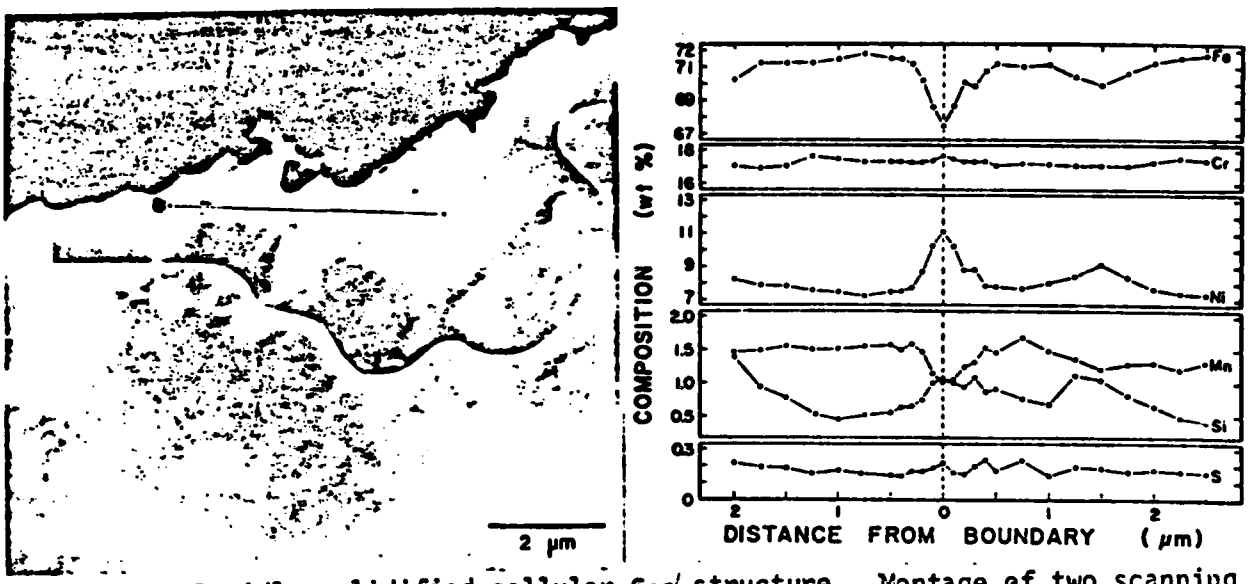

Figure 2 - Rapidly solidified cellular fcc structure. Montage of two scanning transmission electron microscope annular dark-field images and composition profile.

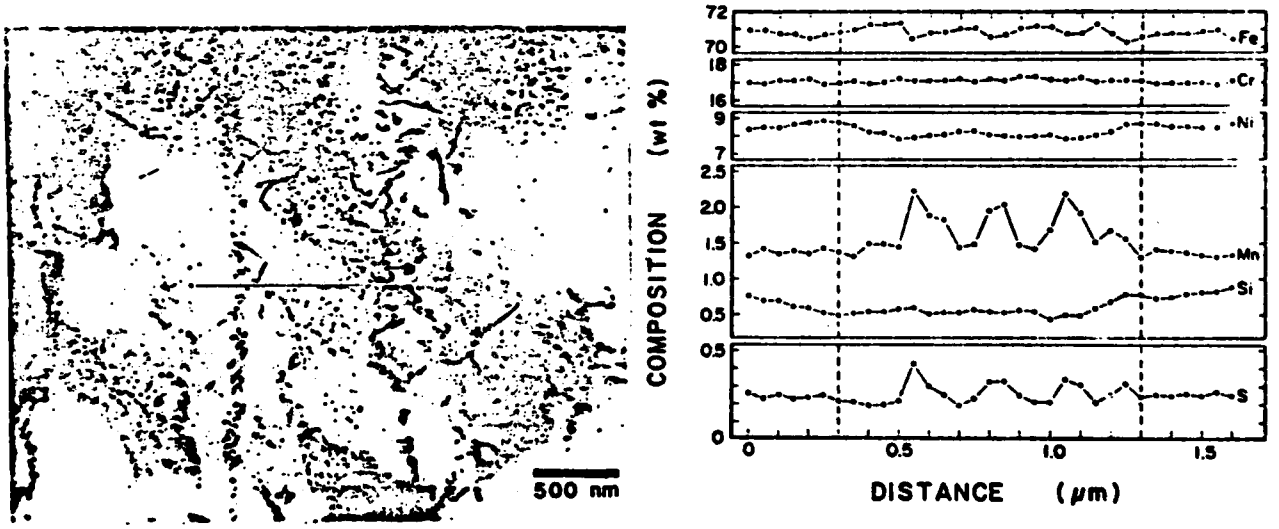

Figure 3 - Rapidly solidified cellular bcc structure. Scanning transmission electron microscope bright-field image and compostion profile.

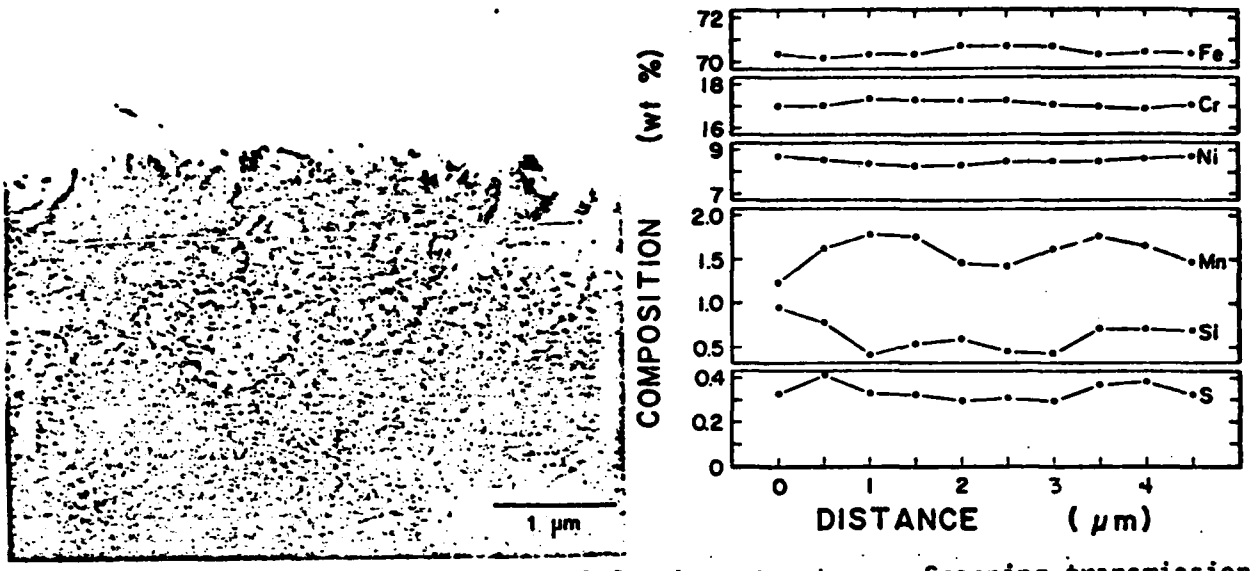

Figure 4 - Rapidly solidified noncellular bcc structure: Scanning transmission electron microscope bright-field image and composition profile.

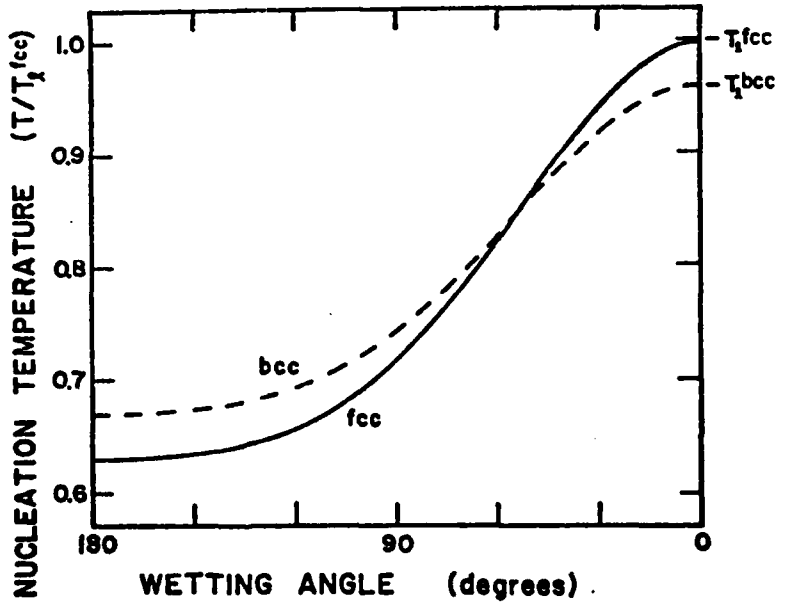

Figure 5 - Schematic plot of the variation of nucleation temperature with wetting angle in heterogeneous nucleation of fcc and bcc for 303 stainless steel. The shapes of the curves are calculated but the value of the bcc liquidus temperature, T_ℓ^{bcc}, relative to the fcc liquidus temperature, T_ℓ^{fcc}, is not known precisely.

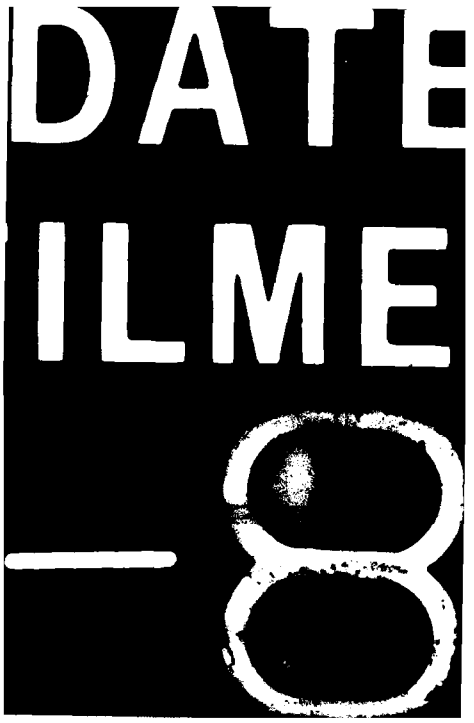
DATE:
ILME
8